

# RF 에너지 하베스팅과 무선 전력 전송에 대한 고찰

민 승 욱\*

## Survey on RF Energy Harvesting and Wireless Power Transmission

Seungwook Min\*

요 약

이 논문은 RF 에너지 하베스팅 (energy harvesting)과 무선 전력 전송 분야에서 현존하는 연구에 대한 기본적인 내용을 제공한다. 주파수, 전력밀도, 수확 전력 등에 기반하여 수확할 수 있는 일상에서 존재하는 RF 전력원들에 대하여 최근의 연구결과를 정리한다. 가까운 거리에서의 무선 전력 전송 (NF WPT)에서는 기본적인 자기유도 방식의 무선 전력 전송 방식을 소개하고, 먼 거리에서의 무선 전력 전송 (FF WPT) 방식에서는 수신기의 안테나와 임피던스 정합 방식을 소개한다. 먼 거리 무선 전력 전송은 수확할 수 있는 상존하는 전력원이 없는 경우에 매우 유용한 방식이다. 가까운 거리 무선 전력 전송 방식은 특히 셀룰러 폰과 같은 이동 단말기 등에 대중화 되어 가고 있다. 무선 전송 방식의 각 부시스템이나 전체 시스템의 효율성을 평가하기 위하여, 효율성과 관련된 측정 단위가 전력비에 의하여 정의된다. 가까운 거리 무선 전송 방식의 구현 방법 중에서, 셀룰러 폰과 전기차를 위한 충전을 이해하기 위하여 자기 유도 커플링 기법과 자기 공명 커플링 기법을 조사한다. 마지막으로, 향후 연구와 전망이 제시된다.

**Key Words** : Radio Frequency (RF), Energy Harvesting (EH), Wireless Power Transmission (WPT), Resonance Coupling, Inductive Coupling

### ABSTRACT

This paper presents a review of existing works in the area of electromagnetic radio frequency (RF) energy harvesting and wireless power transmission (WPT). Ambient RF sources to be harvested are examined based on the frequency band, the power density, and the harvested power. In NF-WPT, the basic magnetic inductive coupling system is examined and the antenna and the impedance matching in receiver system is investigated in FF-WPT. The FF WPT is very useful if there are no ambient energy sources to be harvested. The NF WPT is getting popular especially for the mobile devices such as cellular phones. To evaluate the efficiency of the subsystems and the overall system, the metric related to the efficiency is defined by the power ratio. Among the implementation methods of the NF WPT, we investigate the magnetic inductive coupling technique and the magnetic resonance coupling technique to understand charging for the cellular phones and the electric cars. Common factors in ambient energy harvesting and WPT are the receiver subsystems which contain the antenna, matching circuits, rectifier, and DC to DC converter. Typical and basic structures of the matching circuits and the rectifier are introduced. Finally, future works and the perspectives are suggested.

\* First Author : (ORCID:0000-0003-3080-7510)Sangmyung University, swmin@smu.ac.kr, 정희원  
논문번호 : 201806-C-003-RN, Received May 31, 2018; Revised August 29, 2018; Accepted October 29, 2018

## I. Introduction

The need for the battery free devices is increasing dramatically in many applications including medical and environmental monitoring, electric car charging, wireless sensor networks (WSNs), etc<sup>[1-4]</sup>. For wireless sensor networks, various techniques harvesting different types of energy resources such as solar energy, thermal energy, radio frequency (RF) energy, and piezoelectric energy have been developed. Of these techniques, we particularly focus on the ambient RF energy harvesting (EH) and the wireless power transmission (WPT). The systems harvesting ambient RF energy exploit energy sources already present in the surrounding environments, namely TV, radio, cellular, satellite, and Wi-Fi systems<sup>[5,6]</sup>.

Ambient wireless energy harvesting technologies are generally used for low-power standalone electronics. Energy harvesting from the surrounding RF environments can be a solution to recharge wireless sensor networks. The amount of energy harvested from ambience depends on the type of wireless system deployed close to the harvesting device. The incident power densities and harvested DC power from ambience are summarized in Table 1<sup>[7]</sup>. In the case of wireless LAN (WLAN), the peak power density ranges from 30pW/cm<sup>2</sup> to 13.36μ W/cm<sup>2</sup> with typical transmit power, channel status, and the distance between transmitter and receiver.

If there are no ambient energy sources, wireless power transmission (WPT) can be a powerful technique to recharge devices with the energy needed for their operation<sup>[8]</sup>. The WPT can be divided into two methods near-field (NF) and far-field (FF) WPT, depending on distance between the transmitter and the receiver<sup>[9-11]</sup>. Most of NF-WPT techniques are based on two electromagnetic induction approaches: magnetic induction (or inductive power transfer (IPT)) and electrostatic induction (or capacitive power transfer (CPT))<sup>[12]</sup>. Particularly, the high-power IPT recently emerged as an attractive means for electric car charging. The IPT is able to recharge the devices with low-power level (< 1W) to high-power level (>

1kW)<sup>[13]</sup>. The CPT shares the recharging applications with IPT, such as low-power biomedical devices and mobile devices<sup>[14]</sup>. The FF-WPT is based on magnetic resonance with radio frequency. In RF based WPT, a dedicated power beacon can be used for recharging while data are transmitted simultaneously. Wireless systems in support of simultaneous power and data transfer at different frequency bands are known as out-band system whereas those working at the same frequency bands are known as in-band systems<sup>[10]</sup>.

The remaining parts of this paper are organized as follows. Section II describes the performance metric to measure the efficiency of the WPT systems. Section III investigates the principle of the EH, the NF-WPT and the FF-WPT. Section IV presents the design criteria for the subsystems of the WPT receiver, such as the antenna, the matching circuits, and the rectifier. Lastly, Section V concludes this paper with suggestions for future works.

## II. Performance Metric to Measure Efficiency of RF WPT

Fig. 1 is the block diagram of the FF-WPT systems which consists of 6 subsystems: (1) DC-to-RF conversion, (2) transmit antenna, (3) radio channel, (4) receive antenna, (5) rectifier, and (6) DC/DC conversion<sup>[26]</sup>. In the case of the NF-WPT,

Table 1. Power densities or harvested DC power from ambient RF

Tx band	Peak power density	DC power harvested	Ref.	Year
WLAN	30pW/cm <sup>2</sup>	1.9mW	[15]	2008
WLAN	0.37mW/cm <sup>2</sup>	18mW	[16]	2012
WLAN	0.72mW/cm <sup>2</sup>	76mW	[17]	2012
WLAN	5.1mW/cm <sup>2</sup>	55mW	[18]	2015
WLAN	13.36mW/cm <sup>2</sup>	n/a	[7]	2016
DTV	n/a	60mW	[19]	2009
DTV	n/a	20mW	[20]	2010
DTV	n/a	0.218mW	[21]	2013
GSM1800	35.5mW/cm <sup>2</sup>	0.1mW	[22]	2010
GSM1800	84nW/cm <sup>2</sup>	7.4mW	[23]	2013
GSM900	0.3nW/cm <sup>2</sup>	n/a	[24]	2015
GSM900	1.4mW/cm <sup>2</sup>	n/a	[25]	2016

the radio channel of the FF-WPT corresponds to induction circuit and the receiving antenna is replaced with the resonance circuits<sup>[6]</sup>.

Individual functions of each subsystem are shown in Fig. 1. The overall power transfer efficiency can be expressed as the product of the efficiency of the transmitter, the propagation loss, and the efficiency of the receiver, given as

$$\eta_o = \frac{P_{out}}{P_{in}} = \eta_{transmit} \times \eta_p \times \eta_{receive} \quad (1)$$

where  $P_{out}$  and  $P_{in}$  denote the input DC power and the output DC power, respectively. The efficiency of the transmitter is determined by the DC to RF converter and transmit antenna. To obtain higher transmit efficiency, a beamforming technique providing higher antenna gain can be adopted. The  $P_{tx}$  denotes the output power of DC to RF converter and the  $P_{crp}$  stands for the effective radiated power which is the product of antenna gain and  $P_{tx}$ . Therefore, the transmit efficiency  $\eta_{transmit}$  in (1) can be given as

$$\eta_{transmit} = \frac{P_{tx}}{P_{in}} \times \frac{P_{crp}}{P_{tx}} = \eta_{tx} \times \eta_{ant} \quad (2)$$

For a transmitter-receiver pair, the propagation loss  $\eta_p$  depends on the type of propagation environment, e.g., high-rise business area, low-rise urban area, sub-urban area, rural area, and other type of open area. Through the transmit channel incurring the propagation loss, the  $P_{crp}$  is reduced to the incident power  $P_{inc}$  at the front-end of the receiver. The propagation efficiency  $\eta_p = P_{inc}/P_{crp}$  with typical heights of the transmitting antenna and

receiving antenna is lower in high-rise business area and low-rise urban area, while it is higher with other types of propagation environments.

The efficiency of the receiver can be determined by the three subsystems, as follows

$$\eta_{receive} = \frac{P_{out}}{P_{inc}} = \eta_{rx} \times \eta_{dc} \times \eta_{out} \quad (3)$$

where,  $P_{rx}$ ,  $P_{dc}$  and  $P_{out}$  denote the output power of receiving antenna and impedance matching circuit, the output power of rectifier, and the output power of DC to DC conversion, respectively. The efficiency of each block in the receiver can be computed by constituent efficiencies  $\eta_{rx} = P_{rx}/P_{inc}$  for the antenna and impedance matching circuit,  $\eta_{dc} = P_{dc}/P_{rx}$  for the rectifier, and  $\eta_{out} = P_{out}/P_{dc}$  for DC to DC conversion.

To increase the rectifying efficiency, the receiving antenna must be optimized together with the rectifying circuits<sup>[27]</sup>. An antenna integrated with the rectifier is referred to as a “rectenna”. The output voltage of the rectifying circuit will be too low to directly drive the remaining circuits. Furthermore, the output voltage changes with dynamic input power. Therefore, a DC to DC converter is used to adjust the rectified voltage to the voltage level suitable for an energy storage. The DC to DC efficiency or regulator efficiency is optimized when power management units are included<sup>[28]</sup>.

### III. Principles of Energy Harvesting and WPT

Fig. 2 shows a typical block diagram of an energy harvesting device consisting of the energy source, the power system, and the sensor system. Available types of ambient energy sources in nature include solar energy, thermal energy, ambient RF energy, and piezoelectric energy<sup>[29]</sup>. In the power system, wireless power receiver converts the ambient energy to DC power and stores the converted energy in energy storage devices. The power management unit (PMU) adjusts the power

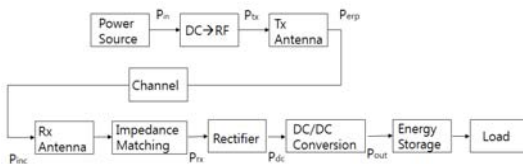


Fig. 1. Block diagram of wireless power transmission system

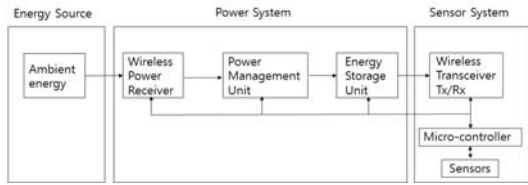


Fig. 2. Block diagram of an energy harvesting wireless sensor system.

level through matching and duty cycle optimization in a power-efficient way<sup>[6]</sup>.

In case of the FF-WPT, the energy source can be replaced with the directed wireless power transmission. The FF-WPT is not gaining popularity so far and thus dedicated frequency band for it has not decided yet<sup>[9]</sup>. Thus, the industrial-scientific-medical (ISM) bands are the only option in prototype development. When transmitting in the license-free ISM frequency bands, the international and domestic transmit power restrictions regulate the transmit power between 10mW and 4W EIRP (equivalent isotropic radiated power), so that it does not exceed the exposure limit<sup>[30]</sup>. For a transmitter-receiver pair in free space, the propagation loss is described by the Frii's power equation<sup>[31]</sup>

$$P_R = P_T \frac{G_T G_R \lambda^2}{(4\pi r)^2} \quad (4)$$

where the  $P_R$  is the received power and the  $P_T$  is the transmitted power and the  $G_T$  is the transmit antenna gain and the  $G_R$  is the receive antenna gain and the  $\lambda$  is the wavelength used and the  $r$  is the distance between the transmit antenna and the receive antenna. For indoor situations, the path loss  $P_L$  may be used instead of the Frii equation in (4)<sup>[32-34]</sup>

$$P_L = 20 \log\left(\frac{4\pi r_o}{\lambda}\right) + 10n \log\left(\frac{r}{r_o}\right) \quad (5)$$

where  $r_o$  is the reference distance, typically 1 meter in indoor environments and  $n$  is path loss exponent.

While the FF WPT is useful for charging the

remote sensors, the NF WPT is becoming popular for the applications<sup>[35]</sup>. The NF WPT can be divided into three classes, zero range, short range, and medium range, according to the distance between transmitter and receiver<sup>[36,37]</sup>. For the zero range or the small gap, the devices can be charged with the conductive mat where the current flows through the pad to a conductive adapter in the device to be charged. For the short range, a device can be charged by the inductive coupling of RF energy when a device with a small receive antenna is placed on a charging surface containing the transmit elements. For medium range, a device is brought within near field of a low frequency transmit antenna. RF energy is coupled with the device via small receive antenna.

Fig. 3 depicts the magnetic induction based circuit networks of the wireless power transmission system as shown in Fig. 1. Among near field wireless power transfer techniques, inductive coupling based WPT is similar to the inductive coupling in transformers<sup>[38]</sup>. Inductive coupling techniques for the WPT use weakly coupled coils which form an air gap transformer between a primary (transmitter) circuit and a secondary (receiver) circuit. Due to the weak coupling through the air between the primary and secondary coils, the efficiency of the transmission is dependent on the shape, the distance between coils, and the materials surrounding both antennas.

Fig. 4 depicts a basic inductively coupled system. The energy is transmitted by an alternating magnetic field from the primary coil to the secondary coil. The efficiency of the transmission is strong dependent on the shape, the distance between the coils, and the materials surrounding both antenna due to the weak coupling through the air between

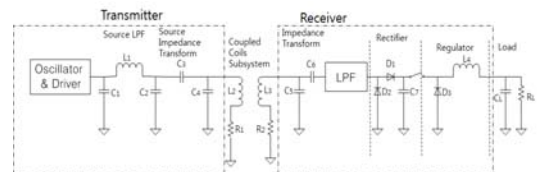


Fig. 3. Magnetic induction based wireless power transfer system.

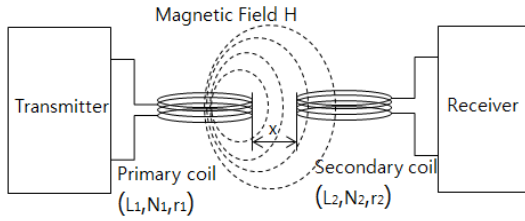


Fig. 4. Typical inductive coupling system

the primary and secondary coils.  $(L_1, N_1, r_1)$  are the inductance, the number of turns and the radius of coil to the primary coil and  $(L_2, N_2, r_2)$  are those to the secondary coil, respectively.

The intensity of the magnetic field at a certain distance  $x$ ,  $H(x)$  can be defined by the following equation<sup>[38]</sup>

$$H(x) = \frac{INr^2}{2\sqrt{(r^2 + x^2)^3}} \quad (6)$$

where  $I$ ,  $N$ , and  $r$  are the current, the number of turns, and the radius of coil, respectively. From Fig. 4, the magnetic field of the transmitter can be maximized by increasing the primary current  $I_1$ , the number of turns  $N_1$  of the transmitting coil or its radius  $r_1$ . The radius of the coil  $r$  is especially interesting to estimate the transmission range of the WPT system. The magnetic field is more or less stable up to a distance of about the radius of the transmitting coil. From this distance, the level of the magnetic field decreases exponentially. Also, the resistances of the transmitter and receiver, frequency dependence such as self-resonance frequency, skin and proximity effects should be taken into account. As a result, the coil size and the number of turns cannot be increased arbitrarily. Therefore, practical

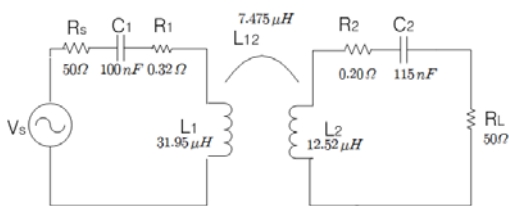


Fig. 5. Equivalent circuit of a two-coil inductive coupling system for WPT

limits exist and they must be optimized in accordance with the chosen transmission frequency.

Simplified equivalent circuit of a two-coil inductive coupling system is illustrated in Fig. 6. In Fig. 6,  $V_s$  is the alternating current power source,  $R_s$  is the resistance in transmitting circuit.  $C_1$  and  $C_2$  are the compensating capacitance of primary and secondary coils, respectively.  $R_1$  and  $R_2$  are the resistances in primary resonator and secondary resonator, respectively.  $R_L$  is the load resistance. The values of each components are the design example<sup>[39,40]</sup>.

Since the magnetic resonance coupling phenomenon is often complicated when it comes down to designing circuits around the resonators, a design and analysis method using an equivalent circuit based on resonator and circuit design is proposed in previous works<sup>[41]</sup>. The WPT through magnetic resonance coupling involves the creation of an LC resonance and transferring the power through magnetic coupling without radiating electromagnetic waves. As shown in Fig. 5, the magnetic coupling can be represented by mutual inductance. The efficiency of the power transfer is calculated based on the equivalent circuit. The power reflection ratio  $\eta_{11}$  and  $\eta_{21}$  the transmission ratio are given as

$$\eta_{11} = |S_{11}|^2 \times 100[\%] \quad (7)$$

$$\eta_{21} = |S_{21}|^2 \times 100[\%] \quad (8)$$

where  $S_{11}$  and  $S_{21}$  represent the wave reflection and transmission ratios, respectively.

The transmission ratio is expressed as

$$S_{21}(\omega) = \frac{2jL_m Z_0 \omega}{L_m^2 \omega^2 + \left[ \left( (Z_0 + R) + j \left( \omega L - \frac{1}{\omega C} \right) \right) \right]^2} \quad (9)$$

The resonance based WPT systems recently reported in the literature have a working frequency of up to few tens of megahertz, while the most typical frequency is around 13.56 MHz<sup>[42]</sup>. Applications for WPT include various areas such as

passive RFID applications, wireless sensors in logistics, structured health monitoring, medical implants, wireless actuators and wireless charging for mobile and electric vehicle applications.

#### IV. Receiver Subsystems for WPT

The receiver subsystems consist of the antenna, the matching circuit, the rectifier and the DC to DC conversion circuit. An essential element for RF application is proper impedance matching to the antenna, since without an impedance matching, much of the power received at the antenna will be reflected back into free space. The received voltage from the antenna via the impedance matching circuit, is insufficient to run a digital IC at the output of the power harvester system. To reach a level usable by digital circuitry, the received signal must be passed through a voltage multiplier which consists of several full wave rectifiers. Thus, we investigate the impedance matching and the rectifier.

##### 4.1 Antenna Impedance Matching

The technological precision of this stage is the most critical in the entire circuit, as even small changes in the resistive or reactive elements of the matching network impedance can cause degradation effects on the efficiency of the antenna reception. Fig. 5 shows the placement of the impedance matching stage. To evaluate the efficiency of the system, two figures of merit, the reflection coefficient and the passive network voltage gain, are defined in<sup>[41]</sup>. The incident power through the antenna is reflected at the rectifier circuit without the matching circuits. The reflection coefficient ensures that the circuit does not radiate power back into free space at the antenna by matching the real and imaginary impedance of the circuit. Impedance matching at the antenna means designing of a network of passive components that transform two mismatched impedances to equivalent ones as shown in Fig. 6. To minimize the reflection coefficient  $\Gamma$  by (10), the matching of the antenna to the rectifier need to be designed efficiently,

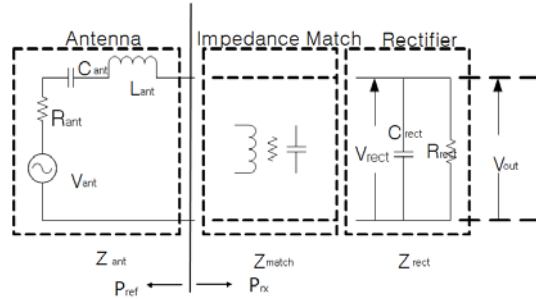


Fig. 6. Schematic impedance matching network

$$\Gamma = \frac{Z_{rect} - Z_{ant}^*}{Z_{rect} + Z_{ant}^*} \quad (10)$$

where,  $Z_{ant} = R_{ant} + X_{ant}$  is antenna impedance,  $Z_{ant}^*$  is its complex conjugate, and  $Z_{rect} = R_{rect} + X_{rect}$  is the input impedance of the rectifier stage. From (9), maximum power transmission will occur when the resistances, or the real part of the impedances are equal, and the reactive components, or the imaginary part of the impedances are of opposite sign. When the reflection coefficient is not zero, the power reflection occurs at the antenna. The fraction of the total power being reflected is quantified as the power reflection coefficient  $|\Gamma|^2$

$$|\Gamma|^2 = \left| \frac{Z_{rect} - Z_{ant}^*}{Z_{rect} + Z_{ant}^*} \right|^2 \quad (11)$$

In Fig 1, the incident power  $P_{inc}$  is reduced to the input power to the rectifier  $P_{rx}$ . That means that some of the incident power at the antenna is received at the rectifier by the value of  $P_{rx}$ , the remainder is reflected at the antenna by the value of  $P_{ref}$ .

$$P_{rx} = P_{inc} - P_{ref} = (1 - |\Gamma|^2)P_{inc} \quad (12)$$

Thus, the efficiency of antenna and the matching circuit  $\eta_{rx}$  ( $=P_{rx}/P_{inc}$ ) is calculated by  $1 - |\Gamma|^2$ .

The purpose of the matching circuit consisted of the LC matching network is to transfer the

maximum power from the antenna radiation resistance ( $R_{ant}$ ) to the resistance of the rectifier ( $R_{rect}$ ) as shown in Fig. 5. LC matching network design should take into account the rectifier parasitic capacitance ( $C_{rect}$ ) resulting from the input capacitance of the active devices used in the rectifier. Once the matching network cancels out the reactive portion of the impedance between  $R_{ant}$  and  $R_{rect}$ , the antenna incident power ( $= V_{ant}^2 / R_{ant}$ ) is shared between  $R_{ant}$  and  $R_{rect}$ . As long as  $R_{rect} > R_{ant}$ , the maximum LC voltage boost (passive network voltage gain) is determined as follows<sup>[42]</sup>,

$$A_{LC} = \frac{V_{rect}}{V_{ant}} \leq \frac{1}{2} \sqrt{\frac{R_{rect}}{R_{ant}}} \quad (13)$$

#### 4.2 Rectifier and Design Example

If a signal has been transformed by the impedance matching network, the rectifier/multiplier of a wireless power harvester serves to both rectify the signal to DC power and boost the voltage from the antenna to a useful level for digital operation<sup>[45-46]</sup>. The simplest implementation of an RF rectifier is shown in Fig. 7. A diode in the half wave rectifier, as shown in Fig. 7a, will conduct and produce a positive voltage across the capacitor, charging the capacitor and providing charge to the output simultaneously, for the positive peak region of the sinusoidal input. For the negative region of the input signal, a diode will cease to conduct and the capacitor will supply all of the charge to the output. Full wave rectifier depicted in Fig. 7b rectifies both the negative and positive regions of the RF signal to provide a more efficient and stable DC output.

These simple rectifiers do not provide any form of voltage gain, and can generate an output DC



Fig. 7. Basic rectifier structure

value proportional to the amplitude of the incoming RF signal. So, rectifiers with a higher number of stages must be implemented by cascading multiple diodes to achieve the voltages necessary for digital operation. Multistage diode can be used to provide higher voltage multiplication, lower the threshold voltage of their first unit, leading to increased sensitivity. However, it should be noted that the added stage components require the cost of higher power losses.

Fig. 8 shows the design example for dipole electrically small antenna (ESA) used in RFID (Radio Frequency Identification) applications. In dipole ESA part, it is a standard  $50\Omega$  antenna which has  $\lambda/10$  length and an impedance  $Z_{feed} = 1.96 - j1758$  ohms. Impedance matching circuit is designed with a Q of 100 for practical application. As a result, the over power conversion efficiency of Fig. 6 is 10%. If the incident power  $P_{incident}$  is  $-16\text{dBm}$  ( $25\mu W$ ), the delivered power to the load is  $2.5\mu W$ .

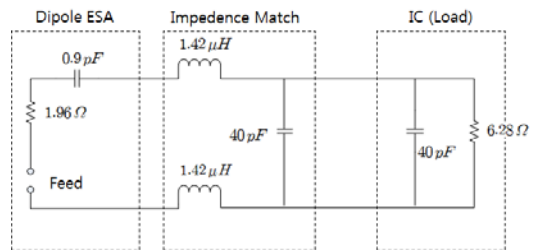


Fig. 8. Design example of the receiver system for WPT

## V. Conclusion

Through the examination of the energy harvesting and WPT, strategy for wireless powering can be established. First, the power density should be assured to support the power to the devices. If there is no enough ambient power, the feasibility of the directed WPT should be considered by means of the transmit frequency, the transmit power amount, the position of transmitter and path loss. Although we concentrate on the RF energy harvesting and WPT, hybrid approaches will be expected the possible solutions for increasing the energy efficiency and the

feasibility.

As the future works, the rectifier technology can evolve by competition of the diode based and CMOS based design. To make WPT feasible and popular, it is required that the new regulation on the transmit power limit, the coverage range, and the effect on health should be established. Especially, the directed WPT is lack of frequency band, so that ISM band is only frequency band for the directed WPT while the ambient energy harvesting obtains the power from DTV, the cellular network, Wi-Fi network and so on.

Beyond the electromagnetic RF ambient/directed powering, other energy can be found in the form of kinetic, chemical, other electromagnetic sources including heat radiation, sun, etc. The future of energy harvesting can be determined by making those energies interacting and exchanged in order to improve efficiency.

## References

- [1] S. Kim, et al., "Ambient RF energy-harvesting technologies for self-sustainable standalone wireless sensor platforms," in *Proc. IEEE*, vol. 102, no. 11, pp. 1649-1666, Nov. 2014.
- [2] F. Habib, et al., "Wireless sensor systems for space and extreme environments: A review," *IEEE Sensors*, vol. 14, no. 11, Nov. 2014.
- [3] C. Souza, et al., "On harvesting energy from tree trunks for environmental monitoring," *Int. J. Distrib. Sensor Netw.*, pp. 1-9, 2016.
- [4] G. Zheng, et al., "An energy supply system for wireless sensor network nodes," *Int. J. Distrib. Sensor Netw.*, pp. 1-6, 2012.
- [5] E. Basha, et al., "UAV recharging opportunities and policies for sensor networks," *Int. J. Distrib. Sensor Netw.*, pp. 1-10, 2015.
- [6] A. Costanzo, et al., "Electromagnetic energy harvesting and wireless power transmission: A unified approach," in *Proc. IEEE*, vol. 102, no. 11, Nov. 2014.
- [7] O. Georgiou, et al., "How many Wi-Fi APs does it take to light a light bulb?," *IEEE Access*, vol. 4, pp. 3732-3746, May 2016.
- [8] M. Pinuela, et al., "Ambient RF energy harvesting in urban and semi-urban environment," *IEEE Trans. Microw. Theory Tech.*, vol. 61, no. 7, pp. 2715-2726, Jul. 2013.
- [9] H. Visser, et al., "RF energy harvesting and transport for wireless sensor network applications: Principles and requirements," in *Proc. IEEE*, vol. 101, no. 6, pp. 1410-1423, Jun. 2013.
- [10] M. Xia and S. Aissa, "On the efficiency of far-field wireless power transmission," *IEEE Trans. on Sign. Process.*, vol. 63, no. 11, Jun. 2015.
- [11] H. Cheng and H. Zhang, "Investigation of improved methods in power transfer efficiency for radiating near-field wireless power transfer," *J. Electrical and Computer Eng.*, pp. 1-11, 2016.
- [12] J. Dai and D. Ludois, "A survey of wireless power transfer and a critical comparison of inductive and capacitive coupling for small gap applications," *IEEE Trans. Power Electron.*, vol. 30, no. 11, Nov. 2015.
- [13] S. Hui and W. Ho, "A new generation of universal contactless battery charging platform for portable consumer electronic equipment," *IEEE Trans. Power Electron.*, vol. 20, no. 3, pp. 620-627, May 2005.
- [14] J. Dai and D. Ludois, "Single active switch power electronics for kilowatt scale capacitive power transfer," *IEEE J. Emerg. Sel. Topics Power Electron.*, vol. 3, no. 1, pp. 315-323, Mar. 2015.
- [15] H. J. Visser, et al., "Ambient RF energy scavenging: GSM and WLAN power density measurements," in *Proc. Eur. Microw. Conf.*, pp. 721-724, Oct. 2008.
- [16] U. Olgun, et al., "Design of an efficient ambient WiFi energy harvesting system," *IET Microw., Antennas Propag.*, vol. 6, no. 11, pp. 1200-1206, Aug. 2012.
- [17] H. Hong, et al., "Demonstration of a highly efficient RF energy harvester for Wi-Fi



- signals,” in *Proc. IEEE Int. Conf. Microw. Millim. Wave Technol.* (ICMMT), vol. 5, pp. 1-4, 2012.
- [18] V. Talla, et al., (2015). “Powering the next billion devices with Wi-Fi,” [Online]. Available: <http://arxiv.org/abs/1505.06815>
- [19] A. Sample and J. R. Smith, “Experimental results with two wireless power transfer systems,” in *Proc. IEEE Radio Wireless Symp.* (RWS), pp. 16-18, Jan. 2009.
- [20] H. Nishimoto, et al., “Prototype implementation of ambient RF energy harvesting wireless sensor networks,” in *Proc. IEEE Sensors*, pp. 1282-1287, Nov. 2010.
- [21] A. N. Parks, et al., “A wireless sensing platform utilizing ambient RF energy,” in *Proc. IEEE Topical Conf. Biomed. Wireless Technol., Netw., Sens. Syst.* (BioWireleSS), pp. 154-156, Jan. 2013.
- [22] D. Bouchouicha, et al., “An experimental evaluation of surrounding RF energy harvesting devices,” in *Proc. Eur. Microw. Conf.*, pp. 1381-1384, Sep. 2010.
- [23] M. Pinuela, et al., “Ambient RF energy harvesting in urban and semi-urban environments,” *IEEE Trans. Microw. Theory Techn.*, vol. 61, no. 7, pp. 2715-2726, Jul. 2013.
- [24] K. Mimis, et al., “Ambient RF energy harvesting trial in domestic settings,” *IET Microw., Antennas Propag.*, vol. 9, no. 5, pp. 454-462, 2015.
- [25] K. Mimis, et al., “The ant and the elephant: Ambient RF harvesting from the uplink,” *IET Microw., Antennas Propag.*, vol. 11, pp. 386-393, 2017.
- [26] Z. Popovic, et al., “Low-power far-field wireless powering for wireless sensors,” in *Proc. IEEE*, vol. 101, no. 6, pp. 1397-1409, Jun. 2013.
- [27] S. Hemour and K. Wu, “Radio-frequency rectifier for electromagnetic energy harvesting: Development path and future outlook,” in *Proc. IEEE*, vol. 102, no. 11, pp. 1667-1691, Nov. 2014.
- [28] V. Marian, et al., “Efficient design of rectifying antennas for low power detection,” *IEEE MTT-S Int. Microwave Symp. Dig.*, pp. 1-4, 2011.
- [29] Y. He, et al., “A survey of energy harvesting communications: Models and offline optimal policies,” *IEEE Comms. Mag.*, vol. 53, pp. 79-85, Jun. 2015.
- [30] E. Falkenstein, et al., “Far-field RF-powered variable duty cycle wireless sensor platform,” *IEEE Trans. Circuits Syst. II, Exp. Briefs*, vol. 58, no. 12, pp. 822-826, Dec. 2011.
- [31] C. A. Balanis, *Antenna Theory, Analysis and Design*, 2nd ed. New York, NY, USA: Wiley, 1997.
- [32] S. Phaiboon, et al., “Upper- and lower-bound path-loss modeling for indoor line-of-sight environments,” in *Proc. Asia-Pacific Microw. Conf.*, vol. 4, 2005.
- [33] S. Duangsuwan, et al., “Experimental study of polarimetric measurement of RFID transfer function within an indoor environment,” in *Proc. IEEE Malaysia Int. Conf. Commun.*, pp. 686-690, 2009.
- [34] S. U. Hwu, Y.-C. Loh, and C. C. Sham, “Propagation characteristics of international space station wireless local area network,” in *Proc. IEEE Radio Wireless Conf.*, pp. 407-410, 2004.
- [35] H. Shoki, “Issues and initiatives for practical deployment of wireless power transfer technologies in Japan,” in *Proc. IEEE*, vol. 101, no. 6, pp. 1312-1320, Jun. 2013.
- [36] The Qi Interface Specification, System Description: Wireless Power Transfer, ver. 1.1.2, *Wireless Power Consortium*, Jul. 2012 [Online]. Available: <http://www.wirelesspowerconsortium.com/downloads/wireless-power-specification>
- [37] M. Kim, et al., “Development of far field RF power harvesting testbed,” *J. KICS*, vol. 40, pp. 1922-1930, Oct. 2015.
- [38] I. Mayordomo, et al., “An overview of technical challenges and advances of inductive wireless power transmission,” in *Proc. IEEE*, vol. 101, no. 6, pp. 1302-1311, Jun. 2013.

- [39] S. Hui, et al., "A critical review of recent progress in mid-range wireless power transfer," *IEEE Trans., Power Electron.*, vol. 29, no. 9, pp. 4500-4510, Sept. 2014.
- [40] Z. Low, et al., "Design and test of a high-power high-efficiency loosely coupled planar wireless power transfer system," *IEEE Trans. Ind. Electron.*, vol. 56, no. 5, pp. 1801-1812, May 2009.
- [41] A. Kurs, et al., "Wireless power transfer via strongly coupled magnetic resonances," *Science*, vol. 317, no. 5834, pp. 83-86, Jun. 2007.
- [42] T. Beh, et al., "Automated impedance matching system for robust wireless power transfer via magnetic resonance coupling," *IEEE Trans. Ind. Electron.*, vol. 60, no. 9, pp. 3689-3698, Sept. 2013.
- [43] T. Soyata, et al., "RF energy harvesting for embedded systems: A survey of tradeoffs and methodology," *IEEE Cir. and Syst. Mag.*, vol. 16, pp. 22-57, 2016.
- [44] N. Soltani and F. Yuan, "A step-up transformer impedance transformation technique for efficient power harvesting of passive transponders," *Microelectron. J.*, vol. 41, no. 2, pp. 75-84, 2010.
- [45] M. Durante and S. Mahlknecht, "An ultra low power wakeup receiver for wireless sensor nodes," in *Proc. 3rd Int. Conf. Sensor Technologies and Applications*, pp. 167-170, 2009.
- [46] G. Vera, et al., "Design of a 2.45 GHz rectenna for electromagnetic (EM) energy scavenging," in *Proc. IEEE Radio and Wireless Symp.*, pp. 61-64, 2010.

민 승 옥 (Seungwook Min)



1987년 2월 : 서울대학교 (공학사)

1990년 2월 : KAIST (석사)

1999년 6월 : Polytechnic Univ. (박사)

2007년 3월~현재 : 상명대학교 컴퓨터과학과

<관심분야> WLAN system 설계, UWB system 설계